Available online at www.sciencedirect.com
SCIENCE DIRECT®
PERGAMON
Deep-Sea Research I 50 (2003) 171–187
DEEP-SEA RESEARCH PART I
www.elsevier.com/locate/dsr

Impact of changing ice cover on pelagic productivity and food web structure in Disko Bay, West Greenland: a dynamic model approach

Anja Skjoldborg Hansen[a,*], Torkel Gissel Nielsen[a], Henrik Levinsen[b], Siz D. Madsen[c], T. Frede Thingstad[d], Benni Winding Hansen[c]

[a] *Department of Marine Ecology, National Environmental Research Institute, PO Box 358, DK-4000 Roskilde, Denmark*
[b] *Freshwater Biological Laboratory, University of Copenhagen, Helsingørsgade 51, DK-3400 Hillerød, Denmark*
[c] *Department of Life Sciences and Chemistry, Roskilde University, PO Box 260, DK-4000 Roskilde, Denmark*
[d] *Department of Microbiology, University of Bergen, Jahnebakken 5, N-5020 Bergen, Norway*

Received 29 November 2001; received in revised form 3 May 2002; accepted 8 October 2002

Abstract

A rise in global temperatures could potentially lead to less ice in the Arctic, including a reduction in the ice-covered period. The consequence of a changing ice cover on the food web structure and production in Disko Bay, Western Greenland, is analysed through application of a dynamical model for the planktonic food web. The model is successfully calibrated and tested for sensitivity, using a detailed data set for 1996–1997. Model scenarios are (1) extended ice cover and (2) no ice. These scenarios are compared to model runs with measured ice cover in two normal years. In the extended ice scenario, assuming unchanged copepod behaviour, copepods are starving or feeding in the ice/water interface from the time they ascend to the surface layer from over-wintering depths until the ice break-up in June. The total annual primary production reaches the same level as it does in the average year, but copepod ingestion and, as a consequence, vertical carbon export is reduced by app. 40%. In the ice-free situation, an early diatom bloom is initiated by stratification of the water in March, before the copepods ascend. The diatom bloom is grazed upon by protozooplankton, which reach a high biomass before the copepods ascend in April. Annual primary production increases by 52% while copepod ingestion and vertical loss of carbon is reduced by 57%. This study illustrates how a change in the ice cover in Arctic areas can potentially create a mismatch between spring primary production and copepod grazers. The result may be a planktonic food web dominated by protozooplankton, resulting in lower export of organic material out of the photic zone despite increased primary productivity, or alternatively lead to changes in species composition or behaviour.

Keywords: Ecological modelling; Environmental impact; Aquatic environment; Food chains; Arctic; West Greenland

*Corresponding author. Present address: Environmental Assessment Institute, Linnésgade 18, DK-1361 K, Denmark. Tel.: +45-72-26-58-05; fax: +45-46-72-58-39.
E-mail address: ash@imv.dk (A.S. Hansen).

0967-0637/03/$ - see front matter © 2003 Elsevier Science Ltd. All rights reserved.
PII: S0967-0637(02)00133-4

1. Introduction

Satellite observations of the Arctic suggest that the area covered with sea ice is decreasing more rapidly than hitherto believed (Johannesen and Miles, 1999; Kerr, 1999). Model studies suggest that the change is due to anthropogenic factors, and that the development in sea ice formation is not likely to reverse (Vinnikov et al., 1999). The extent of arctic multiyear ice has diminished as much as 14% per decade the past 20 years (Johannesen and Miles, 1999).

Marginal seas will presumably be most affected by climatic changes. Based on global circulation models, it was found that a doubling of atmospheric CO_2 would lead to break up of the ice in Hudson Bay, Canada, almost one month earlier than at present (Ingram et al., 1996).

This study is an attempt to assess the changes in a generalised arctic ecosystem subject to global warming. However, regional differences such as changes in the thermohaline circulation may create other changes in specific areas. The western coast of Greenland may experience decreasing temperatures and increasing ice cover in the future (Serreze et al., 2000; Deser et al., 2000).

Previous models of global warming in arctic marine systems have focused primarily on the air–sea CO_2 fluxes and other factors influencing the climatic feedback loops (e.g. Olsson et al., 1999; Slagstad et al., 1999; Tian et al., 2000). Few models have studied the consequences on the marine food web, although planktonic food web structure influences vertical export dynamics of organic matter (Legendre and Rassoulzadegan, 1995). In order to understand the impact of global change on biological productivity as well as CO_2 fluxes, potential food web changes must be addressed. In this study we analyse the consequences of climate changes on pelagic production and consumption rates in a dynamic ecosystem model of the pelagic food web in Disko Bay, West Greenland.

1.1. Study site

The model was calibrated to data collected in Disko Bay (69°15′N, 53°33′W) on the western coast of Greenland at 250 m depth (Fig. 1). The pelagic food web in Disko Bay has been intensively studied during the last decade (Nielsen and Hansen, 1995, 1999; Hansen et al., 1999; Levinsen et al., 1999; Levinsen et al., 2000a, 2000b; Møller and Nielsen, 2000; Madsen et al., 2001). These investigations have documented, in contrast to earlier beliefs, that the structure of the pelagic food web has the same complexity as it does in lower latitude ecosystems, i.e. that bacterioplankton and protozooplankton play an important role. The annual plankton cycle is described in Levinsen et al. (2000a), Madsen et al. (2001) and Levinsen and Nielsen (2002). In brief, the mesozooplankton community is dominated by *Calanus* spp., which are present in the euphotic zone only during a limited period (April–July), after which they migrate to the deep water for overwintering. Usually, the ice break-up takes place in April–May, initiating a diatom bloom. Protozoan grazers respond quickly to the phytoplankton bloom, with high growth rates despite the presence of the large standing stock of copepods that have ascended from their winter hibernation (Levinsen et al., 2000a; Madsen et al., 2001). When most *Calanus* spp. leave the euphotic zone in July, the protozoan biomass as well as the biomass of the small copepod species increases (Levinsen et al., 2000a; Madsen et al., submitted).

The high temporal and vertical resolution of the data from the annual study of Disko Bay makes them suitable for a model calibration. In the present paper, we apply a one-dimensional dynamical model of the planktonic food web to the euphotic zone ($\sim$30 m) of Disko Bay. The goal is to evaluate the consequences of a changing ice cover for the timing between copepod ascendance and the diatom bloom. As copepods have a profound structuring effect on other planktonic organisms, we also want to examine possible effects of a changing ice cover on the general food web structure, productivity and dynamics.

2. Model description

The model used is a dynamical version of a steady-state model described in Thingstad et al.

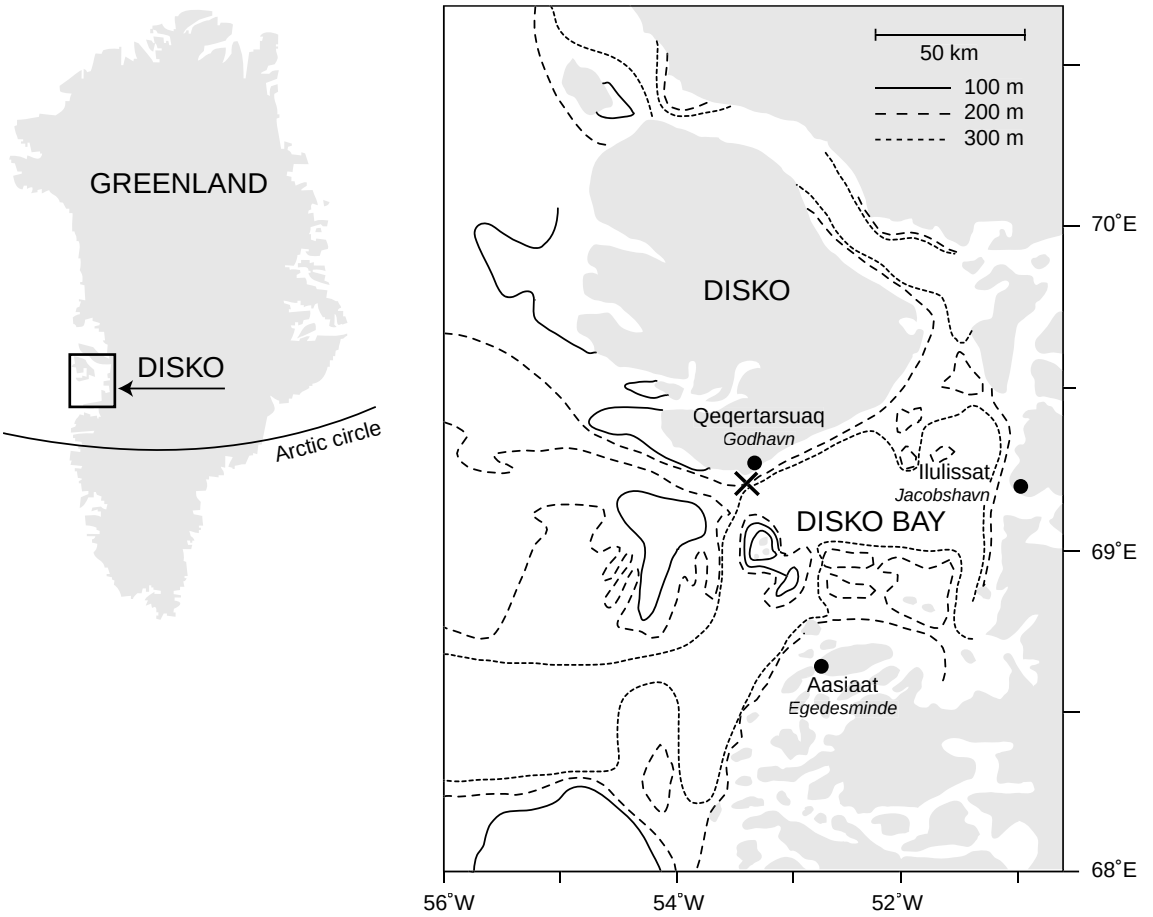

Fig. 1. Map of Disko Bay, West Greenland.

(1997, 1999, 2002). In the original model, the food web consists of bacteria, heterotrophic and autotrophic flagellates, diatoms, ciliates and mesozooplankton.

The present version includes heterotrophic dinoflagellates as grazers on diatoms and ciliates (see Fig. 2). Additionally, ciliates are allowed to graze upon a fraction of the bacteria and diatoms, since previous studies in the area have shown the presence of bacterivorous ciliates (Levinsen et al., 1999, 2000a) and small diatoms (15–20 μm) have been observed in ciliate food vacuoles (Nielsen and Hansen, 1995; Møller and Nielsen, 2000). The magnitude of the trophic coupling between ciliates and these food sources was established through model calibration.

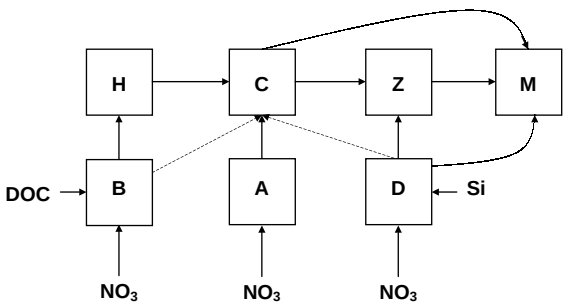

Fig. 2. Diagram of the model food web. A = autotrophic flagellates, B = bacteria, C = ciliates, D = diatoms, H = heterotrophic flagellates, Z = dinoflagellates, M = mesozooplankton, DOC = dissolved organic carbon, Si = silicate.

Nitrogen was the chosen model unit. This nutrient is limiting during summer and is depleted from the surface water before silicate; phosphorus,

on the other hand, is present throughout the year (Nielsen and Hansen, 1995, 1999). Biomass units are $\mu mol\,N\,l^{-1}$ and rates are in $\mu mol\,N\,l^{-1}\,d^{-1}$. Because potential carbon limitation of bacteria and silicate limitation of diatoms are considered, carbon and silicate concentrations are also included as state variables in the model. The forcing variables: water temperature, water density differences, light and ice cover, can be seen in Fig. 3. A list of the abbreviations used in the model is given in Table 1. Differential equations are presented in Table 2.

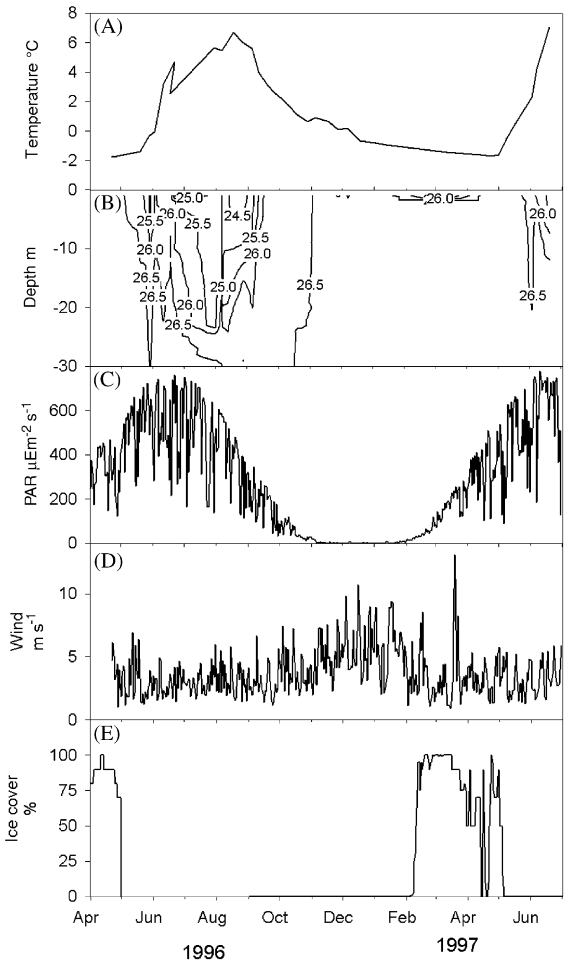

Fig. 3. Model forcing functions. A: temperature (°C) at 2 m depth, B: density profile (σ_t), C: photosynthetic active radiation (PAR, $\mu E\,m^{-2}\,s^{-1}$), D: wind speed ($m\,s^{-1}$) and E: ice cover (%).

Table 1
Abbreviations for state variables and rates

Letter	Name
A	Autotrophic flagellates
B	Bacteria
C	Ciliates
D	Diatoms
H	Heterotrophic flagellates
M	Mesozooplankton
Z	Heterotrophic dinoflagellates
N	Nitrogen pool
DOC	Dissolved organic carbon
Si	Silicate pool
i	Ingestion
d	Death
r	Remineralisation
s	Sinking
u	Uptake
Y	Yield
PAR_{UP}	Photosynthetically active radiation in upper layer
PAR_{LOW}	Photosynthetically active radiation in lower layer
PAR_{IN}	Incoming photosynthetically active radiation at surface

Table 2
Model differential functions

Differential functions
$\frac{dA}{dt} = AuN - CiA - ArN$
$\frac{dB}{dt} = BuN - BrN - HiB - Bd$
$\frac{dC}{dt} = CiH + CiA - CrN - ZiC - MiC - Cd$
$\frac{dD}{dt} = DuN - DrN - Ds - ZiD - MiD$
$\frac{dH}{dt} = HiB - HrN - CiH - Hd$
$\frac{dM}{dt} = MiC + MiD + MiZ - MrN - Mout - Md + Mascent - Mdescent$
$\frac{dZ}{dt} = ZiC + ZiD - ZrN - MiZ$
$\frac{dN}{dt} = ArN + DrN + BrN + HrN + ZrN + MrN - AuN - DuN - BuN + Nadd$
$\frac{dDOC}{dt} = ArC + DrC + BrC + HrC + ZrC + MrC - BuC$
$\frac{dSi}{dt} = ZrSi + MrSi - DuSi + Siadd$

2.1. Physics

The 1-D model describes the upper 30 m of the water column, roughly corresponding to the

euphotic zone (Nielsen and Hansen, 1999). During summer, when the bay was stratified, the model was divided into two layers, upper (up) and lower (low) separated by the pycnocline. Since copepods are able to migrate across the pycnocline, they were not divided between the two layers. The position of the pycnocline was determined from the calculated density profiles (Fig. 3B) and corresponds roughly to the $25.5\sigma_t$ isoline.

Changes in the position of the pycnocline determine the vertical water exchange. A deepening of the mixed layer (ML) associated with increasing turbulent mixing thus transfers nutrients, for example, from the lower to the upper layer. Such events have been documented earlier and are presumably due to wind events (Nielsen and Hansen, 1999). In contrast, state variables become part of the lower layer when the pycnocline moves upwards. It is therefore assumed that the pycnocline is not established by advective processes, and horizontal advection is by necessity considered negligible. This is a simplification, since there is a net transport of surface water out of the bay (Andersen, 1981).

The reduction of light in the water column is described by the light attenuation coefficient. The light is calculated in one-third of the depth of the layer, which is a simplified description of the mean position of a particle moving in the water column. The reflection of light on surface is assumed to be 6% on an ice-free surface and 85% on an ice-covered surface (Kirk, 1994):

$$\mathrm{PAR_{UP}} = \mathrm{PAR_{in}}\, e^{-K_d \mathrm{ML}/3} \times ((1-\mathrm{ice})0.94 + \mathrm{ice} \times 0.15),$$

$$\mathrm{PAR_{LOW}} = \mathrm{PAR_{in}}\, e^{-K_d \mathrm{ML}/3 - K_{dB}(\mathrm{depth}\ B/3)} \times ((1-\mathrm{ice})0.94 + \mathrm{ice} \times 0.15).$$

The light attenuation coefficient is modelled according to Kremer and Nixon (1978). Above the pycnocline:

$$K_d = 0.054 \times \mathrm{chl}\, a^{2/3} + 0.0088 \times \mathrm{chl}\, a + 0.02$$

and below the pycnocline:

$$K_{dB} = 0.054 \times \mathrm{chl}\, a_B^{2/3} + 0.0088 \times \mathrm{chl}\, a_B + 0.02.$$

2.2. Biology and nutrients

Phytoplankton nitrogen uptake and net growth is determined by a maximum N uptake rate, phytoplankton biomass and a temperature function that is modified by nutrient and light limitation functions, modelled with Michaelis–Menten kinetics:

$$\mathrm{AuN} = A V_{\max A} \frac{\mathrm{PAR}}{\mathrm{PAR} + K_{LA}} \frac{N}{N + K_{NA}} Q_{10P}^{(\mathrm{temp}-3)/10}.$$

Silicate limitation is determined by the ratio of silicate supply to maximum silicate uptake. If the supply is limiting, the N uptake becomes dependent on silicate remineralisation:

$$\mathrm{DuN} = \begin{cases} \dfrac{r\mathrm{Si}}{\mathrm{Si}pr\mathrm{N}} \dfrac{\mathrm{PAR}}{\mathrm{PAR} + K_{LD}} \dfrac{N}{N + K_{ND}} Q_{10P}^{(\mathrm{temp}-3)/10}, & \dfrac{r\mathrm{Si}}{\mathrm{Si}pr\mathrm{N} \times D} < V_{\max D}, \\ D V_{\max D} \dfrac{\mathrm{PAR}}{\mathrm{PAR} + K_{LD}} \dfrac{N}{N + K_{ND}} Q_{10P}^{(\mathrm{temp}-3)/10}, & \dfrac{r\mathrm{Si}}{\mathrm{Si}pr\mathrm{N} \times D} \geqslant V_{\max D}. \end{cases}$$

Sinking of diatoms is dependent on the nitrogen concentration:

$$D_s = \begin{cases} \mathrm{Srate}\, D, & N < sT, \\ 0, & N \geqslant sT. \end{cases}$$

Bacteria are limited by either organic carbon (DOC) or nitrogen (N). The affinity (α) for the limiting nutrient determines the growth rate and nitrogen uptake rate:

$$\mathrm{BuN} = \begin{cases} B\alpha_{BN} N Q_{10Z}^{(\mathrm{temp}-3)/10}, & \alpha_{BN} N < \alpha_{BC}\, \mathrm{DOC}, \\ B\alpha_{BC}\, \mathrm{DOC} \times Q_{10Z}^{(\mathrm{temp}-3)/10}, & \alpha_{BN} N \geqslant \alpha_{BC} \mathrm{DOC}. \end{cases}$$

Bacterial carbon uptake (BuC) is calculated from bacterial nitrogen uptake (BuN), assuming a constant carbon efficiency ($\mathrm{BC_{eff}}$) and carbon to

nitrogen ratio for bacteria ($CprN_B$).

$$BuC = \frac{BuN}{BC_{eff}} CprN_B.$$

Bacterial affinity for carbon (α_{BC}) is determined from bacterial affinity for nitrogen (α_{BN}):

$$\alpha_{BC} = \frac{\alpha_{BN} BC_{eff} \times 0.25}{CprN_B}.$$

Ingestion is a saturation function of total prey density, dependent on maximum clearance and maximum ingestion (Holling type II) (Hansen et al., 1997).

The ingestion rate of grazer G feeding on prey P can be described by the function (GiP) for all realised combinations of grazers and prey in the food web:

$$GiP = \begin{cases} \dfrac{GI_{\max G} PQ_{10Z}^{(temp-3)/10}}{(I_{\max G}/Cle_{\max G} + P_{sum})}, & P_{sum} > TG, \\ 0, & P_{sum} \leqslant TG, \end{cases}$$

where G is the biomass of grazer (heterotrophic nanoflagellates (HNF), ciliates, dinoflagellates or copepods), P the biomass prey (bacteria, autotrophic nanoflagellates (ANF), diatoms, ciliates or dinoflagellates), $I_{\max G}$ the maximum ingestion rate for grazer G, $Cle_{\max G}$ the maximum clearance rate for grazer G, P_{sum} the biomass sum of all potential prey sources for grazer G and TG the grazer threshold for feeding.

Remineralisation of nitrogen is determined by the death rate of the producers and the nitrogen yield as well as death rate of the consumers:

$$ArN = dA \times A,$$

$$DrN = dD \times D,$$

$$BrN = dB \times B,$$

$$HrN = (1 - Y_H)HiB + dH \times H,$$

$$CrN = (1 - Y_C)(CiB + CiH + CiA + CiD) + dC \times C,$$

$$ZrN = (1 - Y_Z)(ZiD + ZiC) + dZ \times Z.$$

Copepods produce faecal pellets that can sink out of the euphotic zone prior to remineralisation. Hence only a fraction (0.25, Hansen et al., 1996) of the nitrogen excreted by copepods is remineralised in the model:

$$MrN = (1 - Y_M)(MiD + MiC + MiZ)remN.$$

The rest of the nitrogen is lost to the deeper layers via faecal pellets (*Mout*) see Table 2.

In order to reflect the addition of nitrogen from deeper water, nitrogen was added to the entire water column when the water was fully mixed. The rate of addition was determined by calibration.

DOC is presumably produced locally by remineralisation; thus no organic carbon was added through mixing or advective processes. The producers lose organic carbon when they die. Additionally it is assumed that a constant proportion of the organic carbon produced by photosynthesis is leaked as DOC:

$$ArC = (dA \times A + AuN \times leak)CprN,$$

$$DrC = (dD \times D + DuN \times leak)CprN.$$

Carbon is remineralised by death and excretion from the grazer populations. Excretion equals the respiration loss of carbon, each representing half of the total nutrient losses:

$$BrC = dB \times B\, CprN_B,$$

$$HrC = (0.5HrN + Hd)CprN,$$

$$CrC = (0.5CrN + Cd)CprN,$$

$$ZrC = (0.5ZrN + Zd)CprN,$$

$$MrC = 0.5MrN \times CprN.$$

Net primary production (PP_{net}) is equal to the net N uptake converted to carbon units:

$$PP_{net} = \frac{AuN + DuN}{NprC}.$$

Bacterial production (BP_{net}) is also calculated from the nitrogen uptake:

$$BP_{net} = \frac{BuN}{NprC_B}.$$

2.3. Parameters

Parameter values were allowed to vary within limits of reported literature values. Rate parameters were corrected to 3°C using different Q_{10}

values for zooplankton and phytoplankton (Table 3). Parameter sensitivity was calculated according to Jørgensen (1995) and expresses the relative change in model output divided by relative change in parameter value. Since the model is not linear, the calculated sensitivity depends on the actual level of parameter perturbation. Sensitivity of each parameter was calculated by varying the parameter $\pm 25\%$ and calculating the average resulting relative change in total primary production (S_{pp}) and total copepod ingestion (S_{coping}), representing system productivity and energy transfer to higher trophic levels. The resulting (reduced) formulas then become

$$S_{pp} = \frac{PP_{+25\%} - PP_{-25\%}}{0.5PP_{standard}},$$

$$S_{coping} = \frac{Coping_{+25\%} - Coping_{-25\%}}{0.5Coping_{standard}}.$$

An absolute sensitivity value <1 means that model output response is less than the parameter change. A negative value indicates that the model output is inversely related to the parameter value. Sensitivity values for all the model parameters are in the range of ± 1.

Parameter names, units, values, sensitivities and references are listed in Table 3.

3. Model calibration and validation

The model was run for the calibration period April 22, 1996 to June 6, 1997. Approximately weekly calibration data was available for nutrients, total and size fractionated chlorophyll *a* (Chl $a < 11\,\mu m$ and Chl $a > 11\,\mu m$), primary production and bacterial production (Nielsen et al., in preparation) as well as for the biomass of HNF (Nielsen et al., in preparation), ciliates and heterotrophic dinoflagellates (Levinsen et al., 2000a), and copepods (Madsen et al., 2001). Temperature and salinity forcing data were available for the same dates as biological variables (Nielsen et al., in preparation). Data for daily ice cover and irradiance were provided by Arctic Station, University of Copenhagen (Fig. 3). Model data were converted to carbon units (mg C m^{-3}) according to the Redfield carbon to nitrogen ratio for all groups except for bacteria, which were assigned a carbon to nitrogen ratio of 5 (Fagerbakke et al., 1996). Primary success criteria for calibration were annual integrated rates of primary production and copepod ingestion, determining the overall rate of productivity and trophical transfer.

3.1. Primary producers

For the calibration, the modelled biomasses of ANF and diatoms were compared to the small ($<11\,\mu m$) and large ($>11\,\mu m$) chl *a* size fraction, respectively (Fig. 4A and B). The model underestimates ANF in the deep layer in 1996, and their contribution to the spring bloom in 1997 is somewhat underestimated as well. Diatoms in the upper layer are well modelled, but in the lower layer the model underestimates them. The model thus fails to reproduce the magnitude of the subsurface chl *a* maximum. Modelled primary production is of the right magnitude throughout the season in both strata (Fig. 4C). The timing is good, although the initial peak in production in 1996 is overestimated and the second peak is underestimated. The area-integrated production in the model in 1996 was 38 g C m^{-2}, and the measured production was 26 g C m^{-2} (Nielsen et al., in preparation).

3.2. Heterotrophs

HNF have a low biomass throughout the year compared to model values, which are higher (Fig. 5A). In general, the biomass of ciliates (10–20 mg C m^{-3}) is well described by the model. Ciliates are more abundant than HNF, with a biomass exceeding 50 mg C m^{-3} in late May, which the model fails to predict (Fig. 5B). During late summer, the model also fails to predict increasingly higher levels in the lower layer. Heterotrophic dinoflagellates (H-dino) are modelled well (Fig. 5C). Measurements recorded two blooms of H-dino reaching up to 40 mg C m^{-3}, and these were reproduced in the model.

The total copepod biomass reflected the migration pattern of *Calanus* spp. and reached a

Table 3
Description, unit, value, sensitivity relative to primary production (S_{pp}) and copepod ingestion (S_{coping}) with references

Name	Description	Unit	Value	S_{pp}	S_{coping}	Reference
(*a*) *Bacteria and phytoplankton parameter names*						
$V_{max\,A}$	Maximum N uptake rate, ANF	µmol N µmol N^{-1} d^{-1}	0.5	0.15	−0.15	Sakshaug and Slagstad (1991)
$V_{max\,D}$	Maximum N uptake rate, diatoms	µmol N µmol N^{-1} d^{-1}	0.6	−0.03	0.33	Sakshaug and Slagstad (1991)
K_{NA}	Half saturation for N uptake, ANF	µmol N l^{-1}	0.5	−0.03	0.03	Slagstad and Støle-Hansen (1991)
K_{ND}	Half saturation for N uptake, diatoms	µmol N l^{-1}	0.5	−0.11	−0.07	Slagstad and Støle-Hansen (1991)
K_{LA}	Half saturation for light, ANF	µE m^{-2} s^{-1}	25	−0.06	0.09	Lower limit: 10; Kristiansen and Farbrot (1991)
K_{LD}	Half saturation for light, diatoms	µE m^{-2} s^{-1}	15	−0.31	−0.24	Lower limit: 10; Kristiansen and Farbrot (1991)
Leak	Phytoplankton leak of carbon	Relative to netPP	0.3	−0.07	−0.06	Verity et al. (1991): phaeocystis 20% of grossPP
Si*pr*N	Diatom silicate to nitrogen ratio		1	0.01	0.00	Thingstad et al. (1999)
Srate	Sinking rate for diatoms	m d^{-1}	0.5	−0.23	−0.39	Slagstad et al. (1999)
ST	Nitrogen threshold for diatom sinking	µmol N l^{-1}	1	−0.01	−0.02	Fitted
BC_{eff}	Bacterial carbon efficiency		0.3	−0.17	−0.16	Thingstad et al. (1999)
C*pr*N_B	Bacterial carbon to nitrogen ratio	µmol C µmol N^{-1}	5	0.20	0.16	Fagerbakke et al. (1996)
α_{BN}	Bacterial affinity for nitrogen	l µmol N^{-1} d^{-1}	28.7	0.00	0.00	Thingstad et al. (1999)
(*b*) *Grazer parameter names*						
$Cle_{max\,H}$	Maximum clearance rate, HNF	l µmol N^{-1} d^{-1}	0.5	0.20	0.14	Hansen et al. (1997) (mean 0.5)
$Cle_{max\,C}$	Maximum clearance rate, ciliates	l µmol N^{-1} d^{-1}	1	−0.08	−0.07	Hansen et al. (1997) (mean 0.86)
$Cle_{max\,Z}$	Maximum clearance rate, H-dino	l µmol N^{-1} d^{-1}	1	0.00	−0.04	Hansen et al. (1997) (mean 0.274)
$Cle_{max\,M}$	Maximum clearance rate, copepods	l µmol N^{-1} d^{-1}	0.16	0.11	−0.19	Levinsen et al. (2000) (∼2 ml µgC^{-1} d^{-1})
$I_{max\,H}$	Maximum ingestion rate, HNF	µmol N µmol N^{-1} d^{-1}	2	0.06	0.07	Hansen et al. (1997) (mean 2.5)
$I_{max\,C}$	Maximum ingestion rate, ciliates	µmol N µmol N^{-1} d^{-1}	1.6	0.17	−0.04	Hansen et al. (1997) (mean 0.85)
$I_{max\,Z}$	Maximum ingestion rate, H-dino	µmol N µmol N^{-1} d^{-1}	1.2	−0.01	−0.01	Hansen et al. (1997) (mean 0.54)
$I_{max\,M}$	Maximum ingestion rate, copepods	µmol N µmol N^{-1} d^{-1}	0.36	−0.06	0.32	Hansen et al. (1997) (mean 0.36)
TC	Ingestion threshold for ciliates	µmol N l^{-1}	0.04	0.01	0.00	Fitted

TZ	Ingestion threshold for H-dino	μmol N l^{-1}	0.1	−0.02	0.02	Jakobsen and Hansen (1997)
TM	Ingestion threshold for copepods	μmol N l^{-1}	0.1	0.01	−0.05	Jakobsen and Hansen (1997)
YH	Yield, HNF	μmol N μmol N^{-1}	0.33	0.14	0.18	Hansen et al. (1997)
YC	Yield, ciliates	μmol N μmol N^{-1}	0.33	−0.03	0.01	Hansen et al. (1997)
YZ	Yield, H-dino	μmol N μmol N^{-1}	0.33	0.00	0.00	Hansen et al. (1997)
YM	Yield, copepods	μmol N μmol N^{-1}	0.33	−0.13	0.46	Hansen et al. (1997)
(*c*) *Additional parameter names*						
DA	Mortality ANF	μmol N μmol $N^{-1} d^{-1}$	0.02	0.00	0.00	Fitted
d*B*	Mortality bacteria	μmol N μmol $N^{-1} d^{-1}$	0.01	0.00	0.00	Fitted
d*D*	Mortality diatoms	μmol N μmol $N^{-1} d^{-1}$	0.02	−0.01	0.01	Fitted
d*H*	Mortality HNF	μmol N μmol $N^{-1} d^{-1}$	0.01	0.04	−0.07	Fitted
d*C*	Mortality ciliates	μmol N μmol $N^{-1} d^{-1}$	0.05	−0.03	−0.07	Fitted
d*Z*	Mortality H-dino	μmol N μmol $N^{-1} d^{-1}$	0.03	−0.01	0.01	Fitted
d*M*	Mortality copepods	μmol N μmol $N^{-1} d^{-1}$	0.02	0.07	−0.40	Ohman and Hirche (2001)
A	Relative ciliate predation on bacteria		0.1	0.04	−0.10	Fitted
B	Relative ciliate predation on diatoms		0.25	0.04	−0.10	Fitted
Q_{10P}	Q_{10} for phytoplankton		1.7	−0.20	−0.11	Sakshaug and Slagstad (1991)
Q_{10Z}	Q_{10} for zooplankton		2.8	−0.15	−0.30	Hansen et al. (1997)
C*pr*N	Carbon to nitrogen ratio	μmol C μmol N^{-1}	6.625	Not tested		Redfield ratio
remN	Relative remineralisation of fecal pellets		0.25	0.07	0.05	Fitted

ANF = autotrophic nanoflagellates, HNF = heterotrophic nanoflagellates, H-dino = heterotrophic dinoflagellates.

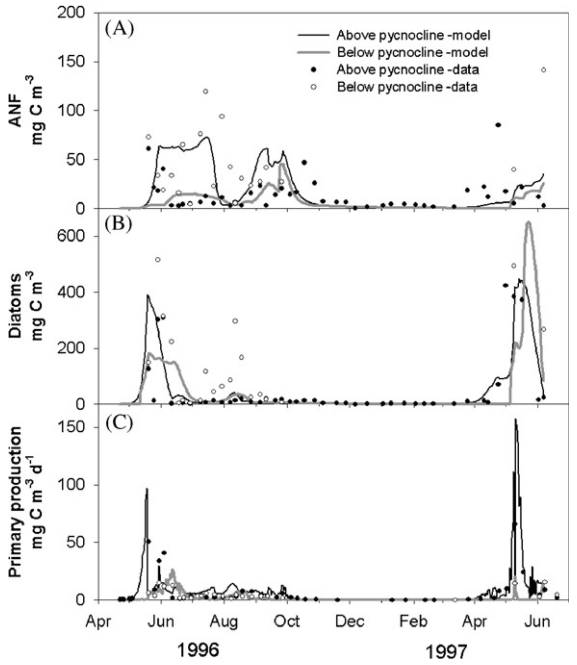

Fig. 4. Modeled and measured values of autotrophic components above and below the pycnocline. A: ANF (mg C m^{-3}), B: diatoms (mg C m^{-3}) and C: primary production (mg C m^{-3} d^{-1}).

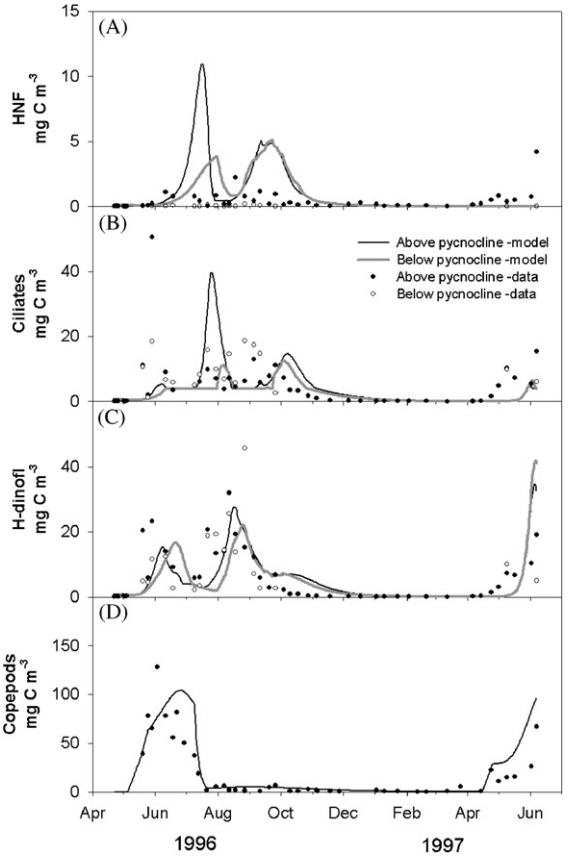

Fig. 5. Modeled and measured values of zooplankton above and below the pycnocline. A: HNF biomass (mg C m^{-3}), B: ciliate biomass (mg C m^{-3}), C: heterotrophic dinoflagellate biomass (H-dino, mg C m^{-3}) and D: copepod biomass (mg C m^{-3}).

maximum of 127 mg C m^{-3} during May 1996, after *Calanus* spp. ascent from the bottom water in April. An abrupt decline in the total biomass was observed in July when *Calanus* spp. descended (Madsen et al., 2001). The *Calanus* spp. migration to and from hibernation was modelled by fit to the measured values. Modelled copepod biomass was of the right magnitude (Fig. 5D). Total modelled copepod ingestion was 12.5 g C m^{-2} in 1996, whereas estimated ingestion was 8 and 14.7 g C m^{-2} based on the egg production method or the temperature-dependent model of Huntley and Lopez (1992), respectively (Madsen et al., 2001).

Measured bacterial biomass varied between 40 and 150 mg C m^{-3} during summer (Fig. 6A). When modelled, the biomass was more constant and only reached 40–80 mg C m^{-3}. Winter levels were modelled correctly. The model underestimated bacterial production, but production responded to the peak in primary production during the spring bloom although a little early compared to measurements.

3.3. Nutrients

Nitrogen was depleted from the upper layer between measurements on May 4 and May 22 (Fig. 7A). In the lower layer, nitrogen removal was slower and nitrogen was not depleted until August. The model correctly describes the use of nitrogen in the upper layer in early May, nitrogen remaining at undetectable levels until mid-September. In the lower layer, the model predicts a slower removal of nitrogen, which stays above detectable

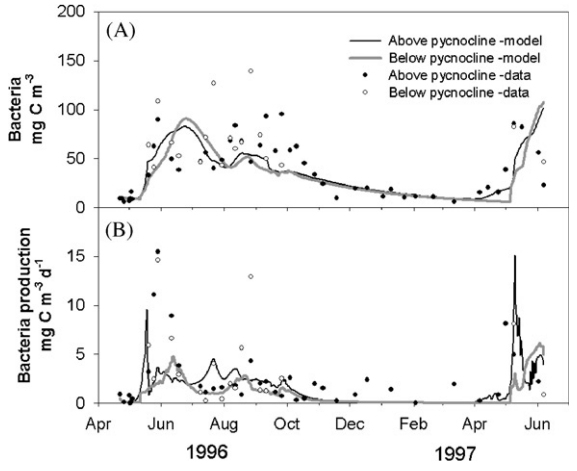

Fig. 6. Modeled and measured values for bacteria above and below the pycnocline. A: bacterial biomass (mg C m^{-3}) and B: bacterial production (mg C m^{-3} d^{-1}).

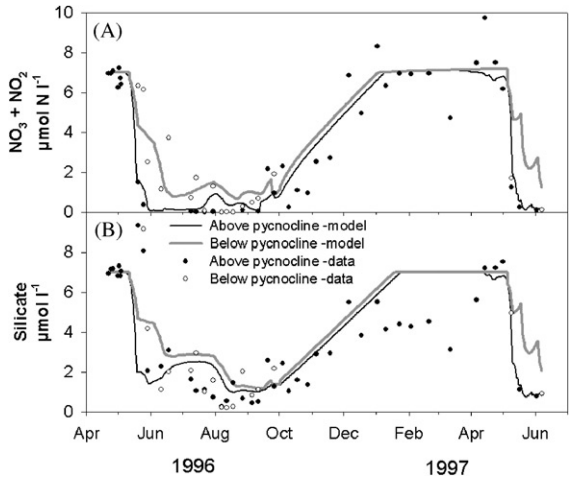

Fig. 7. Modeled and measured values for nutrients above and below the pycnocline. A: nitrogen ($NO_3 + NO_2$, µmol N l^{-1}) and B: silicate (µmol l^{-1}).

levels throughout the stratified period. The model fails to predict complete removal of nitrogen in the lower layer in August. Silicate is removed from the water together with nitrogen in early May (Fig 7B) but remains at detectable levels around 1–2 µmol l^{-1} during the stratification. The removal is slower in the lower layer. The model predicts the correct timing and magnitude of the silicate removal.

3.4. Sensitivity analysis

Sensitivity analysis of all the model parameters was conducted to examine the properties of the model and identify the controlling parameters for primary production and copepod ingestion. Analysis of the sensitivity of the model showed that primary production and copepod ingestion were robust, i.e., not sensitive to a single parameter value. For primary production, parameters for diatom sinking rate and diatom half saturation for light were the major controlling factors. The most positive influence on primary production was from bacterial carbon to nitrogen ratio and HNF clearance on bacteria, indicating a strong competition for nutrients between phytoplankton and bacteria. Copepod ingestion was positively affected by increasing their maximum ingestion and yield but negatively affected by their mortality and diatom sinking rate. Parameters determining the relative competition between autotrophic flagellates and diatoms, such as diatom maximum N uptake and light limitation, also affected copepod ingestion.

4. Model results

4.1. Ice cover scenarios

To test the importance of the timing between the spring bloom and the copepod ascent from hibernation, the model was run for two additional years (1998 and 1999) driven by measured surface irradiance with either (a) measured ice cover, (b) extended ice cover (until June) or (c) no ice cover. These cases were chosen as extremes of future ice scenarios. They were based on the following assumptions: (1) the presence of *Calanus* spp. in the euphotic zone modelled as in 1997 and (2) a simple formulation correlating surface mixed layer depth to irradiance, based on the development in surface mixed layer depth in 1996 and 1997.

Scenario a (measured ice cover, 1997 + 1998): A diatom bloom follows the ice break-up in April–May (Fig. 8A), after the copepods have ascended from their hibernation in April. Ciliates and heterotrophic dinoflagellates respond to the bloom (Fig. 8B and C), but are controlled by copepods

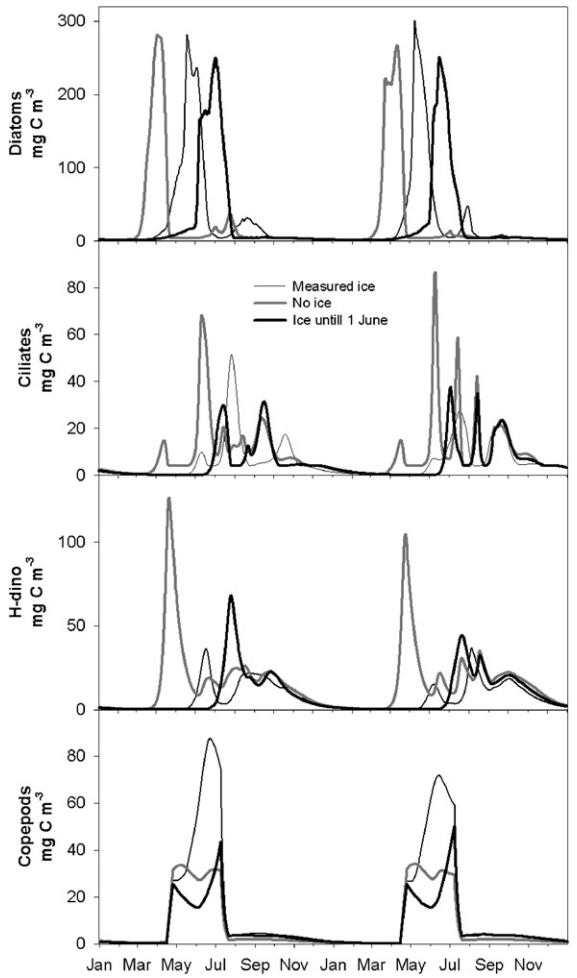

Fig. 8. Model scenarios for 2 years with no, normal and extended ice cover. A: diatom biomass (mg C m^{-3}), B: ciliate biomass (mg C m^{-3}), C: heterotrophic dinoflagellate biomass (H-dino, mg C m^{-3}) and D: copepod biomass (mg C m^{-3}).

until the descent of the *Calanus* spp. Because the copepods are present during the entire diatom bloom period, they ingest 23% of the primary production. Diatoms constitute the majority (77%) of their diet (Table 4).

Scenario b (extended ice cover): This situation represents the extreme ice cover events recorded at the station, e.g. in 1992 (Nielsen and Hansen, 1995). Since the ice first breaks in early June (Fig. 8A), the large copepods are starving from the time of their ascent in April until the diatom bloom in June. They thus obtain a low biomass compared to the situation with measured ice cover (Fig. 8D). Accordingly, the copepod ingestion is only 6.6 g C m^{-2} yr^{-1} or 12% of the primary production (Table 4). The copepods are present throughout the diatom bloom period, and the diatom fraction of the food as well as the annual primary production is unchanged (Table 4).

Scenario c (no ice): In the ice-free scenario, a diatom bloom occurs in association with the formation of a stratified water column in late March (Fig. 8A). Protozoans respond immediately to the bloom, resulting in high ciliate and dinoflagellate biomass levels from mid-April (Fig. 8B and C). As copepods are assumed to ascend from their winter hibernation at a fixed time in late April, when the diatom bloom has sedimented, the protozoans become their major food source (Table 4). The copepod biomass development is low compared to the normal situation (Fig. 8D). The averaged annual primary production has increased from 53.1 g C m^{-2} yr^{-1} at the measured ice cover conditions to 79.7 g C m^{-2} yr^{-1} (Table 4).

Table 4
Integrated primary production and copepod ingestion with changing ice cover

	Ice break April–May	Ice break 1/6	No ice
Primary production	53.1	52.8	79.7
Vertical carbon export	8.2	5.1	3.5
Total copepod ingestion	12.1	6.6	5.3
Copepod ingestion of diatoms	9.2	5.1	0.7
Copepod ingestion of ciliates	1.2	0.5	1.6
Copepod ingestion of dinoflagellates	1.7	0.5	3.0
Copepod ingestion (%) of primary production	23	12	7

All units: C m^{-2} yr^{-1} (average over 2 model runs with forcing data from 1998 and 1999).

The copepod ingestion is decreased from 23% to 7% of the primary production, and the total carbon loss due to sedimentation of diatom cells and copepod faecal pellets is reduced from 8.2 to 3.5 g C $m^{-2} yr^{-1}$ (Table 4). Despite the increased primary production, the net export of carbon is thus reduced by 57% due to lower copepod grazing on diatoms. The remaining organic carbon synthesised by photosynthesis is remineralised in the upper part of the water column.

4.2. Copepod ascent from hibernation

The consequences of changing copepod hibernation duration vs. timing of ice break was explored in a series of model runs, calculating annual copepod ingestion and primary production with forcing for the year 1998 (Fig. 9). The range of copepod ascent is March 27–May 22 (i.e. 4 weeks sooner and later than today). Ice cover varies from March 1 to July 1 (corresponding to 2 months earlier or later than average). The simulated copepod ingestion varies between 3 and 10 g C $m^{-2} yr^{-1}$ (Fig. 9A), and is maximal when the ascent of copepods is matched closely with the ice break. In years with late ice, copepods should ascend as close to the ice break as possible. However, if the ice breaks before March 1, it would be advantageous for the *Calanus* spp. to ascend up to 1 month earlier than today. The present copepod behaviour with ascent in late April is optimal in situations where the ice breaks between April 1 and May 27, thus covering most of the present variation, but not necessarily the assumed future drastic changes. Primary production varies between 40 and 80 g C $m^{-2} yr^{-1}$ (Fig 9B). Primary production is inversely related to copepod total ingestion due to increased grazing pressure, and total area production is maximal when ice break is early and copepods ascend later than today.

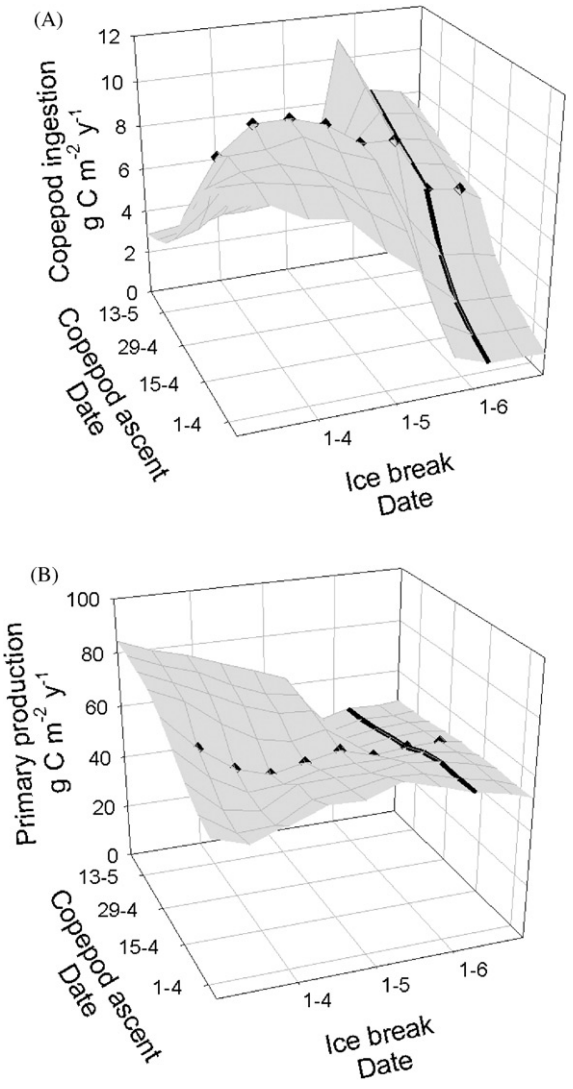

Fig. 9. Model simulations with varying copepod ascent date and ice break date. A: yearly copepod area ingestion (g C $m^{-2} yr^{-1}$); B: yearly area primary production (g C $m^{-2} yr^{-1}$).

5. Discussion

5.1. Model structure and parameters

The main assumption behind a one-dimensional model is the lack of advection. This is a questionable approach in an open system like the Disko Bay, but hydrographical mapping of the Bay has shown that variability in the biological and physical parameters is limited within the Disko Bay basin (Turner et al., 2001; Munk et al., in preparation). Additionally, the surface current velocities are low compared to the coastal areas outside the Bay (Buch, 2000) and the main source of freshwater is diffuse melt water run off rather

than unidirectional river discharge. We therefore consider this system to be less sensitive to advective processes, and thus suitable for a one-dimensional model approach.

One of the probable consequences of rising temperatures is a decrease in the ice-covered period as well as ice thickness in the Arctic. This will greatly increase the irradiation available to the plankton compared to an ice-covered situation. It is uncertain, whether the increased irradiation in an ice-free situation is sufficient to establish a pycnocline in the bay as early as March as suggested by the empiric irradiance vs. mixed-depth model used in the proposed scenarios. The increased temperatures following from global heating, however, will potentially increase melt water runoff. Thus, it is probable that stabilisation of the water column will be possible at an earlier date than at present, whether the stabilising factor is surface heating or salinity differences due to glacier melt water.

Our model contains all major groups of organisms in the planktonic food web, including ciliates and heterotrophic dinoflagellates. Heterotrophic dinoflagellates have not previously been included in arctic food web models as a functional group. Dinoflagellates may however be an important link in the food web, competing with copepods for large phytoplankton while being a food source for copepods as well. Production by algae associated with sea ice was not included in the model, although primary production in the ice–water interface may support a diverse grazer community a few weeks prior to ice break-up (Grastrup-Hansen et al., submitted). This may be an important food source for the copepods until ice-break up and establish a community of protozoan grazers that can immediately exploit the spring bloom. However, the total level of ice algae production is low (Levinsen et al., 2000a), and we consider it to be negligible on a larger scale. Thus, although we have kept the model simple, e.g. by not adding ice algae or mixotrophy, we believe that the included food web is adequate to describe the complex dynamics of the system under changing conditions.

The model was successfully calibrated with data from a study conducted between April 1996 and June 1997 and was able to describe most biomass levels, rates and nutrient concentrations. Importantly, the model was able to simulate the diatom blooms as indicated by the correct prediction of silicate removal in both layers. The high concentration of diatoms in the layer below the pycnocline during summer was not reproduced, however. Because primary production was modelled correctly in this layer, loss rates (grazing and sinking) must have been too high, or the copepods are not homogeneously distributed in the photic zone. Model runs excluding sinking did not increase the biomass substantially. Hence, grazing rates were probably overestimated, as the grazer biomass was of the correct magnitude, or the one-dimensional approach is insufficient to reproduce the main features of biomass established in the pycnocline.

Since the modelled bacterial production is determined by the concentration of DOC, the low production estimates suggest that the production of DOC is underestimated in the model, but this rate is difficult to model correctly in a simple model due to the complexity of the processes involved. Nonetheless, the model prediction that bacterial production was limited by the rate of production of labile DOC is in accordance with earlier findings from Disko Bay (Møller and Nielsen, 2000).

The modelled area primary production in 1996 is 38 g $C\,m^{-2}\,yr^{-1}$. The copepods ingested 12.5 g $C\,m^{-2}\,yr^{-1}$, or 33% of the primary production and 85% of the copepod diet were diatoms. The modelled production lies within the range of reported production from Disko Bay of 36–104 g $C\,m^{-2}\,yr^{-1}$ (Andersen, 1981; Nielsen and Hansen, 1999) and estimates of 20–90 g $C\,m^{-2}\,yr^{-1}$ in the Greenland Sea (Slagstad et al., 1999).

Modelled annual primary production was generally higher in the model in 1997 than 1996, maybe due to a fast increased depth of the mixed layer in spring, possible created by wind events. A deep mixed layer supports a high production since the algae in average experience higher irradiation in the top layer, while the algae in the bottom layer remains trapped below the pycnocline. The development of the pycnocline is thus very important for the modelled total area production, indicating

a close coupling between mixed layer formation and productivity as found in, e.g. Bisset et al. (1994).

The sensitivity analysis showed that bacterial carbon to nitrogen ratio and grazing rates on bacteria were important parameters in determining primary production. The indication that bacteria and phytoplankton are competing for mineral nutrients is not in conflict with the conclusion that DOC production limits bacterial production, but reflects the fact that bacteria have higher nutrient affinity, and thus controls nutrient availability for the phytoplankton. Increased grazing by HNF will thus lead to increased primary production due to a relaxation of bacterial nutrient uptake.

Because of the general low parameter sensitivity, we conclude that the model is robust and can be used to evaluate potential consequences of a changing ice cover.

5.2. Model scenarios

In all the model scenarios, primary production increased with the length of the productive season; thus an early ice break yields most productivity. This is in accordance with the finding of a positive relationship between length of the ice-free period and annual primary production in arctic waters (Rysgaard et al., 1999). We believe that such a higher production is due to more regenerated phytoplankton production. The primary production is, however, also affected by the presence of the *Calanus* spp. In the ice-free situation, the early spring bloom without large copepods present represents a protozoan dominated microbial food web, transferring the primary production through ciliates and/or dinoflagellates before ingestion by copepods. Here, such a situation reduces the vertical carbon fluxes. However, a recent model study in Bonne Bay and Gulf of St. Lawrence indicates that export fluxes may be less dependent on food web structure than concluded here (Tian et al., 2001).

5.3. Resilience of copepod populations

It is not known whether copepods will be able to respond to earlier spring blooms by ascending earlier from hibernation. If the ascent is controlled by photoperiod as suggested by Miller et al. (1991), *Calanus* spp. will not respond to a change in ice cover. If the ascent is controlled by maturation, although at reduced rates, as suggested by Hind et al. (2000), the future hibernation pattern of the large copepods may depend upon the temperature effect of global change at their overwintering depths or possibly their food intake in the previous seasons. If lipid storage determines the ascent, a few years with an early spring bloom would probably reduce their stored reserves due to decreased production, and maybe they would ascend sooner due to starvation. A model study of *Calanus finmarchicus* has shown that minor reductions in food levels lead to severe starvation the following winter due to reduced lipid storage (Fiksen and Carlotti, 1998). Recent studies indicate a large variation in hibernation pattern within the population, indicating large individual variation (Heath, 1999). The variation in response may be due to high genotype variation which may act to ensure adaptation to changing conditions by survival of a few opportunistic individuals in adverse years, resulting in a new population with changed behaviour after a few seasons (Fiksen, 2000). The conclusion holds with day length as the cue for ascent, when inter-annual variation is low. However, variation in ice cover between years may increase in the future in the marginal seas, not allowing the necessary time for adaptation to new environmental conditions.

This study suggests, that if *Calanus* spp. are not able to change the behaviour as a consequence of rising temperatures and match the change in the ice break, the consumers of the primary production will shift from large copepods to heterotrophic dinoflagellates or perhaps small, faster growing, copepod species. Despite increased primary productivity in the system, decreasing copepod production could severely influence copepod predators such as fish larvae and planktivorous fish, thus generating a trophic cascade and eventually influencing the fisheries. Time will show whether ecosystem plasticity and resilience of the large copepod populations are sufficient to respond to dramatic changes in temperature and ice cover without major structural changes.

Acknowledgements

The authors wish to thank Birgit Søborg for technical assistance, Colin Stedmon for linguistic corrections and Dr. Francois Carlotti, Dr. Icarus Allen, Dr. Karsten Bolding and Dr. Mads Peter Heide-Jørgensen for valuable comments on the manuscript. The study was supported by the Danish National Research Council project nos. 9501038 and 9700224. A.S. Hansen was supported by The Danish Research Agency.

The present project also received support from the Danish Environmental Protection Agency as part of Dancea–Danish Cooperation for Environment in the Arctic project #123/001-0259.

References

Andersen, O.G.N., 1981. The annual cycle of phytoplankton primary production and hydrography in the Disko Bugt area, West Greenland. Meddelelser om Grønland, Bioscience 6, 1–65.

Bisset, W.P., Meyers, M.B., Walsh, J.J., Müller-Karger, F.e., 1994. The effects of temporal variability of mixed-layer depth on primary productivity around Bermuda. Journal of Geophysical Research 99, 7539–7553.

Buch, E., 2000. A monograph on the physical oceanography of the Greenland waters. Danish Meteorological Institute Scientific Report, 00-12, Copenhagen.

Deser, C., Walsh, J.E., Timlin, M.S., 2000. Arctic sea ice variability in the context of recent atmospheric circulation trends. Journal of Climate 13, 617–633.

Fagerbakke, K., Heldal, M., Norland, S., 1996. Content of carbon, nitrogen, oxygen, sulfur and phosphorus in native aquatic and cultured bacteria. Aquatic Microbial Ecology 10, 15–27.

Fiksen, Ø., 2000. The adaptive timing of diapause—a search for evolutionarily robust strategies in *Calanus finmarchicus*. ICES Journal of Marine Science 57, 1825–1833.

Fiksen, Ø., Carlotti, F., 1998. A model of optimal life history and diel vertical migration in *Calanus finmarchicus*. Sarsia 83, 129–147.

Grastrup-Hansen, D., Nielsen, T.G., Thomsen, H.A., Buck, K.R., Hansen, B.W. Structure, dynamics of the microbial food web within sea-ice and in the underlying water column during ice-break-up in Disko Bay, West Greenland, submitted for publication.

Hansen, B.W., Flotel, F.L., Jensen, N.J., Madsen, S.D., 1996. Bacteria associated with a marine planktonic copepod in culture. II. Degradation of fecal pellets produced on a diatom, a nanoflagellate or a dinoflagellate diet. Journal of Plankton Research 18, 275–288.

Hansen, P.J., Bjørnsen, P.K., Hansen, B.W., 1997. Zooplankton grazing and growth: scaling within the 2–2000 μm body size range. Limnology and Oceanography 42, 687–704.

Hansen, B.W., Nielsen, T.G., Levinsen, H., 1999. Plankton community structure and carbon cycling on the western coast of Greenland during the stratified summer situation. III. Mesozooplankton. Aquatic Microbial Ecology 16, 233–249.

Heath, M.R., 1999. The ascent migration of *Calanus finmarchicus* from overwintering depth in the faroe-shetland channel. Fisheries Oceanography 8 (Suppl. 1), 84–99.

Hind, A., Gurney, W.S.C., Heath, M., Bryant, A.D., 2000. Overwintering strategies in *Calanus finmarchicus*. Marine Ecology Progress Series 193, 95–107.

Huntley, M.E., Lopez, M.D.G., 1992. Temperature-dependent production of marine copepods: a global synthesis. American Naturalist 140, 201–242.

Ingram, R.G., Wang, J., Lin, C., Legendre, L., Fortier, L., 1996. Impact of freshwater on a subarctic coastal ecosystem under seasonal sea ice (southeastern Hudson Bay, Canada). I. Interannual variability and predicted global warming influence on river plume dynamics and sea ice. Journal of Marine Systems 7, 251–265.

Jakobsen, H.H., Hansen, P.J., 1997. Prey size selection, grazing and growth response of the small heterotrophic dinoflagellate *Gymnodinium* sp and the ciliate *Balanion comatum*—a comparative study. Marine Ecology Progress Series 158, 75–86.

Johannesen, O.M., Shalina, E.V., Miles, M.W., 1999. Satellite evidence for an arctic sea ice cover in transformation. Science 286, 1937–1939.

Jørgensen, S.E., 1995. State of the art of ecological modelling in limnology. Ecological Modelling 78, 101–115.

Kerr, R.A., 1999. Will the Arctic Ocean lose all its ice? Science 286, 1828.

Kirk, J.T.O., 1994. Light and Photosynthesis in Aquatic Ecosystems, 2nd Edition. Cambridge University Press, Cambridge.

Kremer, J.N., Nixon, S.W., 1978. A Coastal Marine Ecosystem: Simulation and Analysis. Ecological Studies. Vol. 24. Springer, Heidelberg.

Kristiansen, S., Farbrot, T., 1991. Nitrogen uptake rates in phytoplankton and ice algae in the barents sea. Polar Research 10, 187–192.

Legendre, L., Rassoulzadegan, F., 1995. Plankton and nutrient dynamics in marine waters. Ophelia 41, 153–172.

Levinsen, H., Nielsen, T.G., 2002. The trophic role of marine pelagic ciliates and heterotrophic dinoflagellates in arctic and temperate coastal ecosystems: a cross-latitude comparison. Limnology and Oceanography 47, 427–439.

Levinsen, H., Nielsen, T.G., Hansen, B.W., 1999. Plankton community structure and carbon cycling on the western coast of greenland during the stratified summer situation. II. Heterotrophic dinoflagellates and ciliates. Aquatic Microbial Ecology 16, 217–232.

Levinsen, H., Nielsen, T.G., Hansen, B.W., 2000a. Annual succession of marine pelagic protozoans in Disko Bay, West

Greenland, with emphasis on winter dynamics. Marine Ecology Progress Series 206, 119–134.

Levinsen, H., Turner, J.T., Nielsen, T.G., Hansen, B.W., 2000b. On the trophic coupling between protists and copepods in arctic marine ecosystems. Marine Ecology Progress Series 204, 65–77.

Madsen, S.D., Nielsen, T.G., Hansen, B.W., 2001. Annual population development and production by *Calanus finmarchicus*, *C. glacialis* and *C. hyperboreus* in Disko Bay, Western Greenland. Marine Biology 138 (6), 1121–1130.

Madsen, S.D., Nielsen, T.G., Hansen, B.W. Annual population development, production by small sized copepods in Disko Bay, Western Greenland: are they neglected contributors? Marine Biology, submitted for publication.

Miller, C.B., Cowles, T.J., Wiebe, P.H., Copley, N.J., Grigg, H., 1991. Phenology in *Calanus finmarchicus*; hypotheses about control mechanisms. Marine Ecology Progress Series 72, 79–91.

Møller, E.F., Nielsen, T.G., 2000. Plankton community structure and carbon cycling off the western coast of Greenland, with emphasis on sources of DOM for the bacterial community. Aquatic Microbial Ecology 22, 13–25.

Munk, P., Hansen, B.W., Nielsen, T.G., Thomsen, H.A. Changes in plankton, fish larvae communities across hydrographic fronts off West Greenland, in preparation.

Ohman, M.D., Hirche, H.J., 2001. Density-dependent mortality in an oceanic copepod population. Nature 412 (6847), 638–641.

Nielsen, T.G., Hansen, B., 1995. Plankton community structure and carbon cycling on the western coast of Greenland during and after the sedimentation of a diatom bloom. Marine Ecology Progress Series 125, 239–257.

Nielsen, T.G., Hansen, B.W., 1999. Plankton community structure and carbon cycling on the western coast of Greenland during the stratified summer situation. I. Hydrography, phytoplankton and bacterioplankton. Aquatic Microbial Ecology 16, 205–216.

Nielsen, T.G, Thomsen, H.A., Hansen, B.W., Levinsen, H., Madsen, S.D. Annual succession of phyto-, bacterioplankton in an Arctic pelagic ecosystem, in preparation.

Olsson, K., Anderson, L.G., Frank, M., Luchetta, A., Smethie, W., 1999. Carbon utilization in the Eurasian sector of the Arctic Ocean. Limnology and Oceanography 44, 95–105.

Rysgaard, S., Nielsen, T.G., Hansen, B.W., 1999. Seasonal variation in nutrients, pelagic primary production and grazing in a high-arctic coastal marine ecosystem, Young Sound, Northeast Greenland. Marine Ecology Progress Series 179, 13–25.

Sakshaug, E., Slagstad, D., 1991. Light and productivity of phytoplankton in polar marine ecosystems: a physiological view. Polar Research 10, 69–85.

Serreze, M.C., Walsh, J.E., Chapin III, F.S., Osterkamp, T., Dyurgerov, M., Romanovsky, V., Oechel, W.C., Morison, J., Zhang, T., Barry, R.G., 2000. Observational evidence of recent change in the northern high-latitude environment. Climate Change 46, 159–207.

Slagstad, D., Støle-Hansen, K., 1991. Dynamics of plankton growth in the Barents Sea: model studies. Polar Research 10, 173–186.

Slagstad, D., Downing, K., Carlotti, F., Hirche, H.-J., 1999. Modelling the carbon export and air–sea flux of CO2 in the Greenland Sea. Deep-Sea Research II 46, 1511–1530.

Thingstad, T.F., Hagstrøm, Å., Rassoulzadegan, F., 1997. Export of degradable DOC from oligotrophic surface waters: caused by a malfunctioning microbial loop? Limnology and Oceanography 42, 398–404.

Thingstad, T.F., Havskum, H., Kaas, H., Lefevre, D., Nielsen, T.G., Riemann, B., Williams, P.J.LeB., 1999. Bacteria–protist interactions and organic matter degradation under p-limited conditions. Comparison between an enclosure experiment and a simple model. Limnology and Oceanography 44, 62–79.

Thingstad, T.F., Nielsen, T.G., Hansen, A.S., Levinsen, H., 2002. Control of bacterial production in cold waters. A theoretical analysis of mechanisms relating bacterial production and zooplankton biomass in Disko Bay, Western Greenland. Marine Ecology Progress Series 228, 15–24.

Tian, R.C., Vézina, A.F., Legendre, L., Ingram, R.G., Klein, B., Packard, T., Roy, S., Savenkoff, C., Silverberg, N., Therriault, J.C., Tremblay, J.E., 2000. Effects of pelagic food-web interactions and nutrient remineralization on the biogeochemical cycling of carbon: a modeling approach. Deep-Sea Research II 47, 637–662.

Tian, R.C., Vézina, A.F., Starr, M., Saucier, F., 2001. Seasonal dynamics of coastal ecosystems and export production at high latitudes: a modeling study. Limnology and Oceanography 46, 1845–1859.

Turner, J.T., Levinsen, H., Nielsen, T.G., Hansen, B.W., 2001. Zooplankton feeding ecology: grazing on phytoplankton and predation on protozoans by copepod and barnacle nauplii in Disko Bay, West Greenland. Marine Ecology Progress Series 221, 209–219.

Vinnikov, K.Y., Robock, A., Stouffer, R.J., Walsh, J.E., Parkinson, C.L., Cavalieri, D.J., Mitchell, J.F.B., Garrett, D., Zakharov, V.F., 1999. Global warming and northern hemisphere sea ice extent. Science 286 (5446), 1934–1937.

Verity, P.G., Smayda, T.J., Sakshaug, E., 1991. Photosynthesis, excretion, and growth rates of phaeocystis colonies and solitary cells. Polar Research 10, 117–128.